

Friction Laws for Elastic Nano-Scale Contacts

L. Wenning and M. H. Müser

Inst. f. Physik, Johannes Gutenberg-Universität, 55099 Mainz, Germany

PACS.81.40.Pg { Friction, lubrication, and wear.

PACS.46.55.+d { Tribology and mechanical contacts.

PACS.07.79.Sp { Friction force microscopes.

Abstract. { The effect of surface curvature on the law relating frictional forces F with normal load L is investigated by molecular dynamics simulations as a function of surface symmetry, adhesion, and contamination. Curved, non-adhering, dry, commensurate surfaces show a linear dependency, $F \propto L$, similar to dry contact on commensurate or amorphous surfaces and macroscopic surfaces. In contrast, curved, non-adhering, dry, amorphous surfaces show $F \propto L^{2-3}$ similar to friction force microscopes. In our model, adhesive effects are most adequately described by the Hertz plus offset model, as the simulations are confined to small contact radii. Curved lubricated or contaminated surfaces show again different behavior; details depend on how much of the contaminant gets squeezed out of the contact. Also, it is seen that the friction force in the lubricated case is mainly due to atoms at the entrance of the tip.

Introduction. { Amontons law, which connects the frictional force F between two solids in relative motion linearly with the normal load L , was suggested more than 300 years ago. This law has proven applicable since for many sliding interfaces [1,2]. Nevertheless, it is still discussed controversially whether or not Amontons' law is valid on the micrometer or the nanometer scale as well, e.g., whether it holds for individual asperity contacts. If a contact deforms plastically, there is a simple popular, yet, phenomenological argument why this should be the case [3]: The local normal pressure p_z in the contact is everywhere close to the yield pressure p_y and the shear stress of the junction is limited through the yield stress τ_c . Omitting adhesive effects, this results in a static friction coefficient of $\mu_s = \tau_c/p_y$. μ_s is commonly defined as the ratio of the force F_s needed to initiate sliding and L . This argument is of rather limited predictive power for various reasons, e.g., p_y depends strongly on the size of the asperities in contact [2]. Furthermore, it can not be applied to elastic, wearless friction, which is the subject of many friction force microscope (FFM) [4{6] and surface force apparatus (SFA) [7,8] experiments. In the following we will focus on wearless, elastic friction.

Even in the elastic regime, SFA and FFM experiments are often consistent with the interpretation of a yield stress τ_c that is (relatively) independent of the normal pressure p_z , e.g., very careful SFA experiments observe that F is mainly proportional to the real area of contact A_c [9]. Similarly, strong deviations from Amontons' laws are observed in FFM. If the FFM tip has a reasonably well-defined shape and adhesive forces are included into the load L in terms of a so-called Hertz-plus-offset model, $F \propto L^{2-3}$ is observed [5]. This is again consistent with the assumption of a normal pressure independent value of τ_c . However, simulations of

friction between μ at surfaces of linear dimensions comparable to FFM contact radii observe Amontons' macroscopic law [10,11] or simple generalizations thereof. The relation between μ_c and p_z is very well described with the linear relation

$$\mu_c = (\mu_0 + p_z \mu_1); \quad (1)$$

where μ_0 can be viewed as an adhesive load per area. $\mu_1 = \partial \mu_c / \partial p_z$ can be interpreted as an differential friction coefficient which is close to $\mu_s = \mu_c / p_z$ in the case of large p_z . Support for the validity of Amontons' law on the microscale has also been provided by SFA experiments in which the adhesive forces between two mica surfaces had been shielded with an electrolyte solution. One may conclude that in typical SFA experiments the term μ_0 dominates $p_z \mu_1$, while in Ref. [8] where adhesive effects were eliminated, p_z dominated μ_0 . Both results are therefore consistent with Eq. (1) and thus consistent with the computer simulations.

It remains to be understood why FFM experiments observe a relationship F / L^{2-3} . The arguments used for the SFA experiments which stresses adhesive effects are not valid for FFM experiments, because the contact mechanics are qualitatively different. Contacts in SFA experiments are usually well described with the JKR model [12], in which a small change in load can change the adhesive interactions considerably. Hence the effective load is typically a highly non-linear function of the externally applied load in an SFA experiment. Due to the much smaller contact radii, FFM experiments are described best by the Hertz-plus-offset model [13]. Here, the adhesive normal forces barely change with the load and simply give a constant bias to the externally applied normal load.

A recently suggested simple model for the interaction between two disordered, but atomistically μ at surfaces predicts a proportionality of μ_c and p_z . However, the net friction coefficient depends on the area of contact A_c according to $\mu_c / p_z = \overline{A_c}$ if no contaminating atoms are present on the surfaces [11]. The predictions of the simple model are then confirmed by detailed atomistic computer simulations [11]. In this letter, we want to show that this relationship explains the observation of the F / L^{2-3} relation seen in FFM experiments: We may regard adhesive forces as an irrelevant offset in FFM and neglect them for a moment. The generalization of the friction law between dry, amorphous, μ at surfaces $F / L = \overline{A_c}$ as suggested in Ref. [11] to curved surfaces and the validity of Hertzian contact mechanics for non-adhesive contacts, in particular A_c / L^{2-3} , automatically lead to the results seen in FFM experiments. We will test this hypothesis by means of molecular dynamics simulation and investigate the friction force of a curved tip on a μ surface as a function of surface symmetry (commensurate, incommensurate, amorphous), adhesion (adhesive, non-adhesive) and contamination of air-born particles, which may alter frictional forces significantly in both experiment [14] and simulation [10,11,15].

The model. { The model used in this study is similar to that used in many previous studies, e.g., Refs. [10,16]: Atoms in each solid are coupled elastically to their ideal lattice positions. Interactions between atoms from opposing walls are Lennard Jones (LJ) interactions. Additional lubricant atoms (if present) interact with one another and with all wall atoms via LJ potentials, namely $V = 4 \left[\left(\frac{\sigma}{r} \right)^{12} - \left(\frac{\sigma}{r} \right)^6 \right]$. Unlike usually, we will not express the results in reduced LJ units but rather give them "reasonable" dimensions of $\sigma = 3 \cdot 10^{-11}$ m and $\epsilon = 3.5$ eV. There is one important new feature in the model, which allows for long-range elasticity orthogonal to the interface. The basic idea is similar to the one used in a recent computer simulation study of the squeezing out of lubricants between a curved and a μ surface [17]. In this letter, the tip atoms are coupled to their ideal, stress-free positions in such a way that the ideal Hertzian pressure profile is generated if the tip is pressed on a perfectly μ at, infinitely hard, and non-adhering surface. This can be achieved simply by using a normal



Fig. 1 { Free amorphous tip (left) with $R_c = 7$ nm and the same tip pressed against a flat (invisible) surface with a load of $L = 40$ nN (right). The flattened area can be interpreted as the area of contact. The tip is shown up-side down in order to improve visualization.

restoring force

$$f(z) = \frac{P}{z=K} - \frac{P}{R_c} \quad (2)$$

with z the normal deflection from the ideal lattice position, R_c the radius of curvature of the tip, and K the bulk modulus of the tip, which was typically chosen $B = 25$ GPa. The equilibrium positions are given by a function that is sinusoidal in x and y direction and periodic with the length of the simulation box L_{box} . R_c is therefore a function of the height h of the tip and L_{box} . A typical amorphous tip is shown in Fig. 1 at zero and maximum externally applied load. The pressure free tip has a height of about $h = 11$ Å. The lateral linear dimension of the simulation box shown is 125 Å.

Results. { We first consider the case of dry surfaces and suppress the effect of thermal activation by choosing extremely small temperatures. Furthermore, adhesive effects between the walls are eliminated by cutting off the LJ potential in the minimum. Three different tips are simulated, (i) one tip commensurate with the substrate, (ii) the same tip as in (i) but rotated by 90° resulting in incommensurability, and (iii) a tip with a disordered structure which we call amorphous. Eliminating thermal activation and suppressing adhesion allowed us to observe the load-friction behavior down to very low normal loads with large resolution, i.e., we know the pull-off force to be exactly zero. The static friction force F_s vs. load L curves are shown in Fig. 2.

The results can be interpreted as follows: (i) For commensurate surfaces, all tip atoms in the contact are basically "in phase", that is to say their lateral positions with respect to the

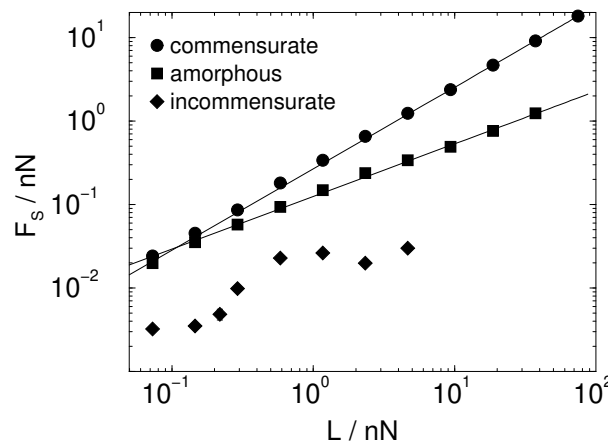


Fig. 2 { Static friction force F_s vs. normal load L for a commensurate tip, an incommensurate tip, and an amorphous tip. In all three cases, the contact radius was $R_c = 70$ Å. The contacts were non-adhesive. Straight lines are fit according to F_s / L .

underlying substrate are identical (modulo the lattice constant). From atom-atom commensurate surfaces, we have learned that on the atomic scale $F_{\text{lateral}}^{(\text{atomic})} / L^{(\text{atomic})}$ is rather well satisfied [11]. The linearity F / L for commensurate tips is therefore not surprising. However, care has to be taken. This analysis is premature: Depending on the local normal pressure, atoms are detected differently in their lateral positions. If we plot individual contributions to the friction force as a function of the load that individual atoms carry, no linearity is observed, but rather f_i / l_i with f_i the lateral force and l_i the normal force that one atom of the tip exerts on the lower wall and $\alpha = 2/3$. Yet, the net friction force $\sum_i f_i$ is proportional to the net load $\sum_i l_i$. The mechanism how this comes about is very much related to a Greenwood-Williamson type argument [18]. (ii) The amorphous tip can be fitted best with a power law $F / L^{0.63}$, which is very similar to the relation predicted in the introduction and seen in FFM experiments. The sublinear behavior can therefore be explained with an increasingly geometric mismatch between the tip and the substrate with increasing load. We have to emphasize that the results shown in Fig. 2 are the result of a statistical average over twelve tips. Individual force-load curves do typically not result in such smooth curves. The relative large contact radii in real AFM tips may already lead to some kind of self-averaging as compared to our simulations. All our tips have been prepared under identical "experimental" conditions, however, the tips have been cut out from different regions of an amorphous solid. (iii) Incommensurate walls show a systematic increase in F vs. L only at very small contact radii, where basically one atom is in contact. As the load is increased, the incommensurability becomes more and more important and the ratio $F=L$ decreases dramatically. The intermittent behavior very much depends on the relative number of tip atoms which are in phase with the substrate. This results in non-trivial $\alpha(A_c)$ behaviour, although the large A_c limit is of course zero.

If we allow for adhesion between the surfaces (by choosing a large cut-off radius), no qualitative changes of the above stated results can be expected. This can be seen by calculating the so-called Tabor parameter, which tells us what contact mechanics model is the most appropriate. [5,19] Even if we use the smallest, physically meaningful value for the tip's bulk modulus and the largest contact radius tractable with the present computer resources, we would still be in the Hertz-plus regime.

We now consider the case of physisorbed atoms or molecules on the surfaces. These contaminating particles may be air-born or a boundary lubricant. For a discussion of mechanisms how several layers of lubricant get squeezed out of the contact see Ref. [17]. In order to discuss the effect of the physisorbed particles on the net shear force of the junction, it is instructive to visualize the distribution of normal loads and shear forces that individual tip atoms experience. This is done in Figs. 3 and 4, where it is shown which tip atoms contribute to friction and which tip atoms carry the normal load (Fig. 3). In Fig. 4, a cross section of the junction is visualized. The center of the tip is in direct contact with the lower wall. There is a large normal pressure in that area, but the lateral forces are fairly small. More load-carrying tip atoms can be found at the center of the ring associated with a single monolayer lubrication regime. It is noticeable that only atoms at the entrance contribute to the friction forces, while atoms at the exit of the tip being located in a geometrically similar position barely carry any load. The tip atoms at the exit even experience a force from the tip atom in the direction of the externally applied load. This can change if adhesive interactions are present as well. Note that real surfaces - depending on the chemical composition - may be prone to cold weld or to generate some kind of debris. Here, however, we want to confine ourselves to the case of chemically passivated surfaces and elastic contacts in order to single out the effect from the lubricant.

In the remaining calculations, adhesive effects were again reduced by making the interac-

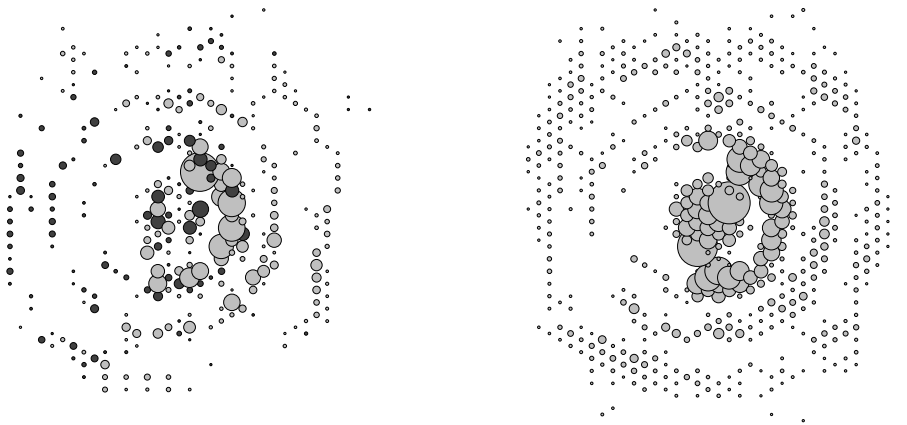


Fig. 3 { Left: Lateral force f on individual tip atoms exerted by the opposite wall and the lubricant. The size of the particles is proportional to $|f|$. Light atoms resist the externally applied force F_{ext} , dark atoms support F_{ext} . Right: Normal force l on individual tip atoms exerted by the opposite wall and the lubricant. The size of the particles is proportional to l .

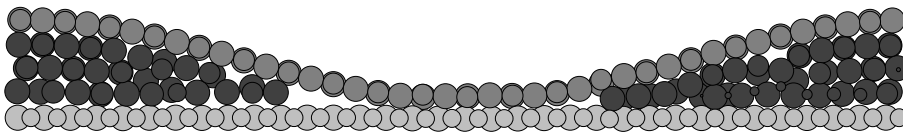


Fig. 4 { Visualization of the lubricated junction. The walls are incommensurate; the external force acts to the right. In the center, all of the lubricant (dark atoms) is squeezed out.

tion of tip atoms with substrate atoms and the lubricant purely repulsive. The only attractive interactions take place between lubricant and substrate so that the substrate is wetted. We have made sure that traces in the fluid film on the substrate induced through scraping of the tip heal sufficiently fast before the tip has been moved for one periodic image. In Fig. 5, force-load curves are shown for a system consisting of a clean crystalline tip on a contaminated, incommensurate surface. Sublinear behavior is found, namely $F / L^{0.85}$. This can be interpreted in such a way that the center of the tip which is in direct contact with the substrate does not contribute to frictional forces while the lubricated areas behave similarly as boundary lubricated, flat surfaces which show F / L [10]. The net force results from the superposition of both effects. Of course, in real experiments the chemical nature of the lubricant will be relevant as well, i.e., the power law relating F_s and L has been observed to depend on the external conditions [20]: Different laws for a Si_3N_4 tip on mica were obtained in argon gas and ambient conditions.

Conclusions. { This study shows that dry, elastic friction between a curved tip and a flat substrate can be perfectly understood from the frictional behavior of dry, flat interfaces: Commensurate systems show linearity between the friction force F and the load L for both curved and flat interfaces. If one of the two surfaces is amorphous, F / L is still valid for a flat interface. The friction coefficient, however, depends on the area of contact according to $\mu_s / 1 = \overline{A_c}$. Assuming the validity of Hertzian contact mechanics, this leads to a $F / L^{2=3}$

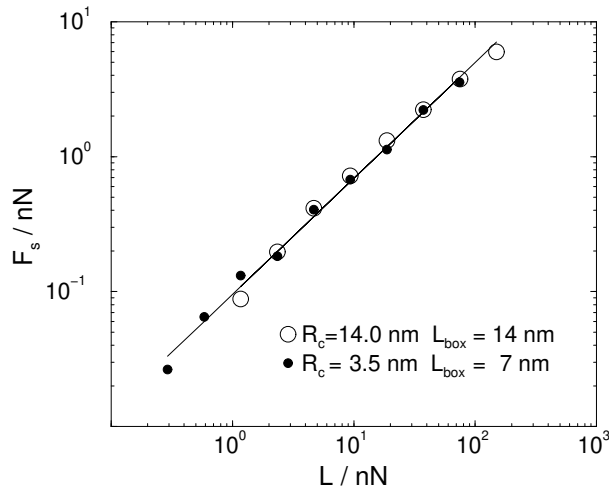


Fig. 5 Static friction force F_s vs. normal load L for an incommensurate tip on contaminated surface for two different contact radii R_c and length of simulation box L_{box} . The straight line reflects a fit with a power law F_s / L with $\alpha = 0.85$.

dependency for curved contacts. This has been confirmed by computer simulations using disordered surfaces and including the effect of long-range elasticity. The validity of Hertzian contact mechanics has been imposed by using purely repulsive potentials. Incommensurate, flat surfaces do not show friction at all. For curved surfaces, friction is therefore only seen if A_c is very small and the ratio F_s/L quickly decreases with increasing contact radius.

Contaminated and lubricated surfaces are more difficult to understand. For flat surfaces, previous simulations have shown that Amontons' laws are well satisfied – including the observation that F_s does not depend on the area of contact. However, as explicitly shown for incommensurate tip-substrate systems, very much depends on the wetting and the squeezing out properties of the lubricant. At the point of direct contact between tip and substrate, the systems are not fully equivalent to the dry case, because the load is not only carried at the center of the tip, but also further outside, where lubricant atoms decrease the effective distance between substrate and tip. These "outskirts" do not only carry load but also contribute significantly to the net friction force. Thus, the friction-load law results from an interplay of the tribological properties of the direct contact and the (boundary) lubricated contact. Depending on the details such as wetting and squeezing properties of the lubricants, different friction-load laws can be expected. In this study, we have observed a $F_s / L^{0.85}$ dependence of a boundary-lubricated incommensurate tip-substrate system, which we do not believe to be universal for this kind of system.

We thank K. Binder, B.N.J. Persson, and M.O. Robbins for useful discussions. M.H.M. is grateful for support through the Israeli-German D.I.P.-Project No 352-101.

REFERENCES

- [1] Dowson D., History of Tribology (Longman Inc., New York) 1979.

- [2] Persson B.N.J., *Sliding Friction: Physical Principles and Applications* (Springer, Berlin) 1998.
- [3] T. Baumberger, *Physics of Sliding Friction*, edited by Persson B.N.J. and Tosatti E. (Kluwer, Dordrecht) 1996.
- [4] Mate C.M., McClelland G.M., Erlandsson R. and Chiang S., *Phys. Rev. Lett.*, 59 (1987) 1942.
- [5] Schwarz U.D., Zworner O., Koster P. and Wiesendanger R., *Phys. Rev. B*, 56 (1997) 6987.
- [6] Schwarz U.D., Zworner O., Koster P. and Wiesendanger R., *Phys. Rev. B*, 56 (1997) 6997.
- [7] Israelachvili J.N., *Surf. Sci. Rpt.*, 14 (1992) 109.
- [8] Berman A., Drummond C. and Israelachvili, *Tribol. Lett.*, 4 (1998) 95.
- [9] P. McGiggan, *Tribology on the 300th Anniversary of Amontons' Law*, edited by D. M. D. and Robbins M.O. (MRS, Warrendale) 1999.
- [10] He G., Muser M.H. and Robbins M.O., *Science*, 284 (1999) 1650.
- [11] Muser M.H., Wenning L. and Robbins M.O., *cond-mat/0004494* (2000).
- [12] Johnson K.L., Kendall K. and Roberts A.D., *Proc. R. Soc. London A*, 324 (1971) 301.
- [13] Schwarz U.D., Bluhm H., Holscher H., Allers W. and Wiesendanger R., *Physics of Sliding Friction*, edited by Persson B.N.J. and Tosatti E. (Kluwer, Dordrecht) 1996.
- [14] Martin J.X., *Phys. Rev. B*, 48 (1993) 10583.
- [15] Muser, M.H. and Robbins M.O., *Phys. Rev. B*, 64 (2000) 2335.
- [16] Thompson P.A., Robbins M.O. and Grest, *Israel J. of Chem.*, 35 (1995) 93.
- [17] Persson B.N.J. and Ballone P., *J. Chem. Phys.*, 108 (1997) 6996.
- [18] Greenwood J.A. and Williamson J.B.P., *Proc. Roy. Soc. A*, 295 (1966) 300.
- [19] Tabor D., *J. Colloid Interface Sci.*, 58 (1977) 2.
- [20] Putman C.A.J., Igarashi M. and Kaneko, R., *Appl. Phys. Lett.*, 66 (1995) 3221.